PCCP

ROYAL SOCIETY OF CHEMISTRY

PAPER

View Article Online
View Journal | View Issue

Cite this: *Phys. Chem. Chem. Phys.*, 2021, **23**, 2731

Insights on the catalytic behaviour of sulfonic acid-functionalized ionic liquids (ILs) in transesterification reactions – voltammetric characterization of sulfonic task-specific ILs with bisulfate anions†

María B. Martini, [a] José L. Fernández *[ab] and Claudia G. Adam *[a]

Received 30th October 2020,
Accepted 15th January 2021

DOI: 10.1039/d0cp05674j

rsc.li/pccp

This work shows for the first time the link between the amount of free sulfuric acid (as detected by cyclic voltammetry) and the activity of sulfonic-acid-functionalized ionic liquids (ILs) as acid catalysts for a transesterification reaction, and demonstrates that sulfonic acid groups, while are not directly involved in the catalysis, release the free acid during the reaction. Two imidazolic ILs with bisulfate as the counterion and their corresponding task-specific ILs (TSILs) that resulted from the addition of a sulfonic acid group inside the imidazolic-base structure were studied. The outstanding catalytic activity at room temperature of the TSILs 1-(4-sulfonic acid)-butyl-3-methylimidazolium bisulfate (**[bsmim]HSO$_4$**) and 1-(4-sulfonic acid)-butyl-imidazolium bisulfate (**[bsHim]HSO$_4$**) for the transesterification of *p*-nitrophenyl acetate with methanol was associated to the significant amounts of free sulfuric acid in equilibria with the ionic pairs. It was concluded that these TSILs function as reservoirs for releasing the free acid, which is the actual acid catalyst. In contrast, the corresponding non-sulfonic ILs supply very little amounts of free acid and consequently present low catalytic activities at room temperature, which in fact can be improved by increasing the reaction temperature up to 100 °C.

Introduction

The fascinating properties of ionic liquids (ILs) opened up a huge range of new research areas spanning different branches of Chemistry and Physics.[1–3] In organic synthesis, ILs have been classified as "*green solvents*" due to their high physicochemical stability, low volatility, tunable solubility, and easy recyclability.[4–6] These properties are being increasingly exploited for simplifying existing synthesis methods and/or for designing new environmentally benign processes.[7,8] ILs also fit into the category of "*designer solvents*", as their physicochemical properties can be modulated by the combination of a vast variety of cations and anions. Moreover, ILs can be specifically designed for accomplishing a particular task by introducing functional groups inside their chemical structures. In these ILs, known as "task-specific ionic liquids" (TSILs),[9–12] the functional groups are incorporated into the cationic bases in order to modify a specific property that directs the IL behaviour for accomplishing a predefined specific task in a reacting system. In particular, the incorporation of sulfonic acid functional groups (SO_3H) leads to TSILs with strong Brønsted acid properties, which are specially useful when using the counterion HSO_4^- for acid catalysis in esterification and transesterification reactions.[13–16] These properties turned sulfonic-based TSILs into excellent alternative solvents and catalysts in processes for biodiesel synthesis.[17–19] This dual solvent/catalyst role played by TSILs in these applications shows that they can be much more than just green solvents.

For the design of TSILs, it is important to understand, at least in some extension, the mechanism of its performance. This is key information for proposing modifications of the main IL structure with functional groups toward a specific goal. However, an aspect that is at the same importance level and cannot be ignored is that the method used for the IL synthesis determines the species that may be naturally present within the IL. In many cases, the precursor reactants that were used to form the ionic pairs remain within the liquid.[20,21] These

[a] *Instituto de Química Aplicada del Litoral (IQAL, UNL-CONICET) and Facultad de Ingeniería Química, Universidad Nacional del Litoral, Santiago del Estero 2829 (3000) Santa Fe, Argentina. E-mail: jlfernan@fiq.unl.edu.ar, cadam@fiq.unl.edu.ar*

[b] *Programa de Electroquímica Aplicada e Ingeniería Electroquímica (PRELINE), Facultad de Ingeniería Química, Universidad Nacional del Litoral, Santiago del Estero 2829 (3000) Santa Fe, Argentina*

† Electronic supplementary information (ESI) available: Structures of bases and zwitterions, additional cyclic voltammograms, additional UV-vis spectra, details on their processing, calibration curves, mechanistic details and kinetic calculations. See DOI: 10.1039/d0cp05674j

are either spontaneously generated by natural equilibrium,[22] or just cannot be removed during purification without reversing the IL synthesis reaction. This particular issue results critical because it may be the reason of some specific behaviours of the ILs that determine their performances. For example, it was recently reported that alkylammonium-derived ILs synthesized by acid–base addition contain the acid and base precursors in autoprotolysis equilibrium with the ionic pairs.[23] The particular combination of ions and neutral species determines the properties of the synthesized IL, and then its performance in an application is influenced by all the interactions that are established within the reactive system.

In this context, our interest is to contribute to the design of imidazolic TSILs relating the structural modifications performed on the cationic bases of the ILs with their chemical compositions and behaviours as solvents and acid catalysts. The Brønsted acid properties of ILs are governed by the different functional groups within their structures that can function as proton donors. Thus, in principle one way to modify the acid properties should be through the incorporation of a sulfonic acid group in the cationic imidazolic structure. On this direction, four ILs with imidazolic bases and bisulfate counterion (two of them never reported) were synthesized and evaluated (see Table S1 in the ESI†). Two of them were sulfonic-type TSILs, where the imidazolic-base structures 1-methyl-3-buthylimidazolium (**[bmim]**) and 1-buthylimidazolium (**[bHim]**) were decorated with SO_3H groups, leading to 1-(4-sulfonic acid)-butyl-3-methyl-imidazolium (**[bsmim]**) and 1-(4-sulfonic acid)-butyl-imidazolium (**[bsHim]**) cations, and to the resulting **[bsmim]HSO$_4$** and **[bsHim]HSO$_4$** TSILs. In addition, the corresponding ILs without the SO_3H groups in the base structure were synthesized for comparison, leading to **[bmim]HSO$_4$** and **[bHim]HSO$_4$**, respectively. In this way, we tuned the Brønsted acid properties of these TSILs, not only by incorporating a SO_3H group (as explained previously), but also by adding other potentially labile proton sources in the imidazole base structure of **[bHim]** and **[bsHim]** cations. The goal of this analysis is to shed some light on the role of the SO_3H group that is present in the TSIL structure in its global performance over a reactive system. As it is described in the literature, this performance might be governed by many structure-dependent variables such as the specific and non-specific interactions that may take place between catalyst, reactants and products, as well as the solubility, the stability, among others.[1,24,25] However, as this performance also depends on the global composition of the IL, in this work this composition was monitored by cyclic voltammetry.

Electrochemical techniques are being intensely used for exploiting the outstanding properties of ILs as electrolytes,[26] and particularly cyclic voltammetry has shown to be extremely useful as a detection technique for revealing the presence of free species other than the ionic pair.[21,23] Thus, in this work the monitoring of ILs by cyclic voltammetry was carried out in order to perceive the effect of the IL synthesis conditions and parameters (synthesis reaction time, purification steps) on the amounts of these species. Our hypothesis is that a specific behaviour of a sulfonic TSIL in a reactive system cannot be attributed solely to the presence of the SO_3H groups that functionalize the TSIL structure. There are many other variables (structural and compositional) that may affect the IL response, so it should be quite difficult to extend its behaviour to other similar ILs, even in the same family. This could be one of the reasons for the significant dispersion of results on the activity of these systems that is found in the literature. On the other hand, even though it is well known that the counterion also affects the catalytic properties of ILs, in this work the counterion HSO_4^- was kept constant in all the analyzed ILs because this is one of the most commonly used anions in these imidazolic combinations. The effect of changing the counterion will be analyzed in a following report. Finally, the catalytic performances of these four ILs were tested in a transesterification reaction by monitoring the reactant consumption and buildup of product concentration by UV-vis spectroscopy, which allowed the estimation of yields at different reaction times.

Experimental

Chemicals and materials

Imidazole (Him), methyl imidazole (mim), butyl bromide, 1,4-butanesultone, sodium ethoxide, *p*-nitrophenyl acetate, sulfuric acid (97–98%), and sodium bisulfate used as precursors or reactants were from Sigma-Aldrich. Methanol, sulfuric ether, ethyl acetate, hexane, acetone, butyl alcohol, and dichloromethane used as solvents or eluents were from Sigma-Aldrich. 1-Butyl-imidazole (bim) was synthesized by reaction of imidazole with butyl bromide through an aliphatic nucleophilic substitution, following a previously reported method that employs sodium ethoxide for deprotonating the imidazole,[27,28] as it described in the ESI.†

Instrumentation

UV-vis spectra were taken using a Shimadzu UV-1800 UV/visible spectrophotometer. Voltammetric experiments were carried out using a CH Instruments CHI1140B potentiostat.

Synthesis of sulfonic TSILs

The TSILs **[bsmim]HSO$_4$** and **[bsHim]HSO$_4$** were synthesized by reaction of sulfuric acid with the corresponding zwitterions, which are listed in Table S2 in the ESI.† Thus, the syntheses of these TSILs involved two steps: (i) the synthesis of the respective zwitterions; (ii) the protonation of the sulfonic groups at the zwitterions to obtain the cations of the final TSILs.

Syntheses of zwitterions 4-(1-methylimidazolium-3-yl)-1-butane sulfonate (Zbsmim) and 4-(1-imidazolium-1-yl)-1-butane sulfonate (ZbsHim). Zbsmim and **ZbsHim** were synthesized by reaction of the corresponding imidazole (Him or mim) with 1,4-butanesultone, as it is sketched in reaction (1).

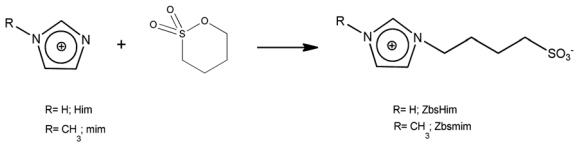

(1)

These syntheses were carried out by mixing 0.05 mol of the corresponding imidazole and 0.05 mol of 1,4-butanesultone dissolved in 7 mL of methanol (MeOH) into a round bottom

flask under reflux and agitation, during 12 h at 68 °C for **Zbsmim** and during 72 h at 35 °C for **ZbsHim**. After these reaction times, the mixtures were vacuum evaporated at 70 °C for 2 h. The precipitation of a white solid was verified for **Zbsmim**, and a whitish viscous liquid was formed for **ZbsHim**. The purification of these products was performed by successive washing steps using sulfuric ether as solvent. While **Zbsmim** was pure enough after these washing steps, for **ZbsHim** it was necessary to apply a recrystallization step in an ice bath. The re-crystallized **ZbsHim** was further re-dissolved in 5 mL of MeOH, and received the dropwise addition of ethyl acetate (10 mL). This solution was finally evaporated under vacuum at 65 °C for 1 h. Both zwitterions were hygroscopic white solids that were dried under vacuum for 48 h and stored in nitrogen atmosphere. Both the reaction and the purification process were monitored by silica gel TLC employing hexane/ethyl acetate (2 : 1) as eluent. Besides, the purification process was monitored by UV-vis spectroscopy.

Synthesis of TSILs by neutralization of zwitterions with H_2SO_4. In order to obtain the TSILs with bisulphate as counter-ion, both zwitterions were neutralized with sulfuric acid through reactions (2) and (3).

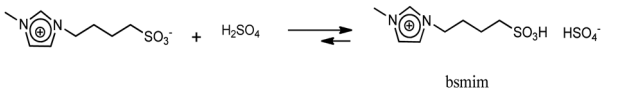

bsmim

(2)

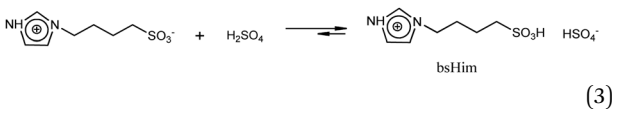

bsHim

(3)

The neutralization steps for both TSILs were carried out in a two-neck round bottom flask under reflux and agitation. A solution with 0.05 mol of the corresponding zwitterion (**ZbsHim** or **Zbsmim**) in 5 mL of MeOH was reacted with 0.05 mol of H_2SO_4 for 20 h at 40 °C. The reaction was monitored by silica gel TLC using as eluents acetone/MeOH (1 : 1) for **[bsmim]HSO$_4$** and hexane/ethyl acetate (1 : 2) for **[bsHim]HSO$_4$**. In both cases the reaction product was a light yellow viscous liquid, which was placed in rotary evaporator for 1 h at 65 °C. The purification involved two extraction steps, first with butyl alcohol and then with sulfuric ether, a step under rotary evaporator for 2 h, and a final drying step at RT under ultra-high vacuum for 48 h.

Syntheses of the imidazolium-based ILs

Synthesis of [bmim]HSO$_4$. The IL **[bmim]HSO$_4$** was obtained by an exchange reaction between **[bmim]Br** (synthesized as described in a previous report[29]) and $NaHSO_4$, as it is shown in reaction (4).

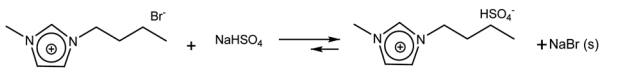

(4)

A solution with 0.05 mol of **[bmim]Br** and 0.05 mol of $NaHSO_4$ in MeOH (6 mL) was heated at 68 °C for 72 h in a round bottom flask under reflux and agitation. The exchange was monitored by silica gel TLC using hexane/ethyl acetate (2 : 1) as eluent. The solid NaBr that precipitated during the exchange reaction was separated by vacuum filtration. The supernatant viscous liquid was placed in rotary evaporator at 65 °C for 2 h to remove MeOH. It was finally dried under vacuum for 48 h, acquiring a light yellowish orange colour.

Synthesis of [bHim]HSO$_4$. The IL **[bHim]HSO$_4$** was obtained by direct protonation of bim (obtained as described in the previous section[27,28]) with H_2SO_4, as indicated in reaction (5), by reacting 0.05 mol of bim dissolved in MeOH (5 mL) with 0.05 mol of H_2SO_4 added slowly into a two-neck round bottom flask under reflux and agitation at 40 °C for 20 h.

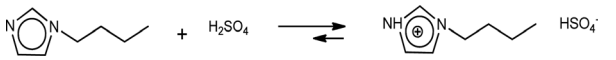

(5)

The reaction was monitored by silica gel TLC using acetone/MeOH (1 : 1) as eluent. The reaction product was a light yellow viscous liquid, which was placed in rotary evaporator at 80 °C for 2 h. Then it was purified by several extractions with sulfuric ether, brought to rotary evaporator for 2 h, and dried under ultra-high vacuum for 48 h.

Transesterification reaction

The model reaction that was used to evaluate the acid catalytic performance of the analyzed ILs was the transesterification reaction (or alcoholysis) between *p*-nitrophenyl acetate (**PNPA**) and MeOH giving 4-nitrophenol (**PNP**) and methyl acetate, according to reaction (6). This type of reaction, where an ester of a carboxilic acid is converted into a different one, can be displaced toward products with complete conversion by using an excess of alcohol (reactant) and an efficient acid or basic catalyst.

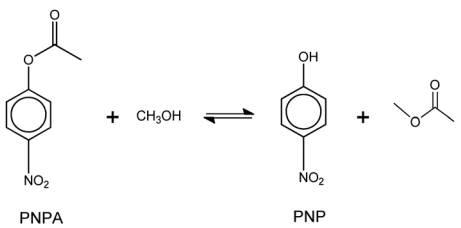

PNPA PNP

(6)

The mechanisms and kinetics of transesterification reactions under homogeneous acid catalysis conditions is an old topic[30] still under discussion.[31–34] The reaction proceeds through a typical nucleophilic substitution in the acyl carbon. The most accepted pathway for primary and secondary alcohols (which is sketched in Scheme S1 of the ESI†) involves the ester protonation and further nucleophilic addition of MeOH to the carbonyl carbon leading to a tetrahedral intermediate. The last steps involve the acyl C–O bond cleavage of the intermediate and consequent elimination of **PNP**. When using protic ILs and TSILs as acid catalysts, the required protons could be provided by different sources located both within the molecular structures of the ionic pairs (such as the SO_3H group in TSILs, the imidazolic hydrogen, and the bisulfate counterion) and at the free species (such as sulfuric acid) that remain in autoprotolysis equilibrium with the ionic pair.

The reaction was carried out into a quartz cuvette (2 mL) thermostatted at the desired reaction temperature, starting from a **PNPA** solution in MeOH with a **PNPA** concentration $C^{\circ}_{PNPA} = 0.1$ mM and an IL concentration of 0.1 M. For comparison of the performance against a well-known catalyst (as is sulfuric acid), this reaction was also carried out using 0.1 M H_2SO_4 instead of the IL. Most of the evaluations were done at 25.0 ± 0.1 °C, although some experiments were carried out at 60.0 ± 0.1 °C and at 100.0 ± 0.1 °C. The course of the reaction was monitored by UV-vis spectroscopy by acquiring spectra of the reaction media over the wavelength range between 220 and 500 nm every pre-defined time intervals. The **PNP** concentrations (C_{PNP}) were estimated using these spectra taken at different reaction times (t_R) from the absorbances measured at 310 nm, and using calibration curves measured on standard solutions of **PNP** in MeOH containing the respective ILs (see the ESI† for details on this procedure). This allowed the calculation of the reaction yields $\left(100 \times C_{PNP}/C^{\circ}_{PNPA}\right)$ at different t_R values.

Voltammetric experiments

The synthesized ILs were characterized by cyclic voltammetry of Pt microelectrodes (MEs) for detecting free electroactive species (*i.e.* IL's parent species, or other species remaining from the synthesis). These experiments were carried out as described elsewhere.[23] Briefly, a thermostatted low-volume (3 mL) three electrode cell was employed, with a disk-shaped 25 μm-diameter Pt ME as working electrode,[35] and a Pt wire as counter-electrode. The reference electrode was a PdH wire[36,37] placed inside a Luggin–Habber capillary that contained the same cell electrolyte. For operation, the cell was loaded at RT with the IL and closed with the Teflon cap that supported all the electrodes. Then, in order to melt those ILs that were solid, the cell temperature was raised to 80 °C. The resulting volume of the melted IL was ~1.5 mL. The electrolyte was purged with inert gas (dry N_2) by continuous bubbling. Cyclic voltammograms (CVs) were measured over a range of potentials (E) from a cathodic enough value (where reduction of the IL cation[38] and/or hydrogen evolution[23,37] was verified) to an anodic value where the oxidation of an IL component was detected, at a scan rate (v) of 0.1 V s^{-1}. In order to confirm the assignment of voltammetric waves to the reduction or oxidation of a specific free species, when possible, pure precursors (*i.e.* **[bmim]Br** and zwitterions) were added during the experiments by using a canister placed at the cell cap. The absence of voltammetric peaks that could be associated to the reduction of platinum oxide formed from water traces allowed to confirm the inexistence of water at detectable levels.[39,40]

Results and discussion

Voltammetric analysis of [bmim]Br and [bmim]HSO_4

Imidazolic ILs with **bmim** as cation and with two different counterions (bromide and bisulfate) were analyzed first. As can be seen in the molecular structure of **bmim** (Table S1, ESI†), the imidazole has a H atom at the C atom in position 2 (which *a priori* should be the most labile H in **bmim**), and other less-labile H atoms at the C atoms in positions 4 and 5. Hydrogen atoms at the saturated carbon atoms in methyl and butyl substituent are hardly labile. The cathodic behaviours of ILs with this cation are very relevant for identifying the possible sources of protons at the imidazolic base that may be able to participate in processes with acid catalysis. The onset potentials of the observed cathodic voltammetric waves for H_2 discharge from the different H atoms indicate how easy should be to draw on these proton sources. Moreover, as the bisulfate counterion is also a potential proton donor, the IL with bromide anion as counterion was analyzed first to identify the exclusive reduction of protons from the **bmim** cation.

The CV of a Pt ME in **[bmim]Br** is shown in Fig. 1a. The anodic profile shows an exponential grow of the anodic current at $E > 0.3$ V, which never arrives to a limiting value (blue curve). This indicates that this current was generated by the oxidation of a large amount of reactant. Thus, it is most likely associated to the oxidation of bromide anions that form part of the IL ionic pair, generating bromine. In addition, an oxidation voltammetric peak is detected over the potential

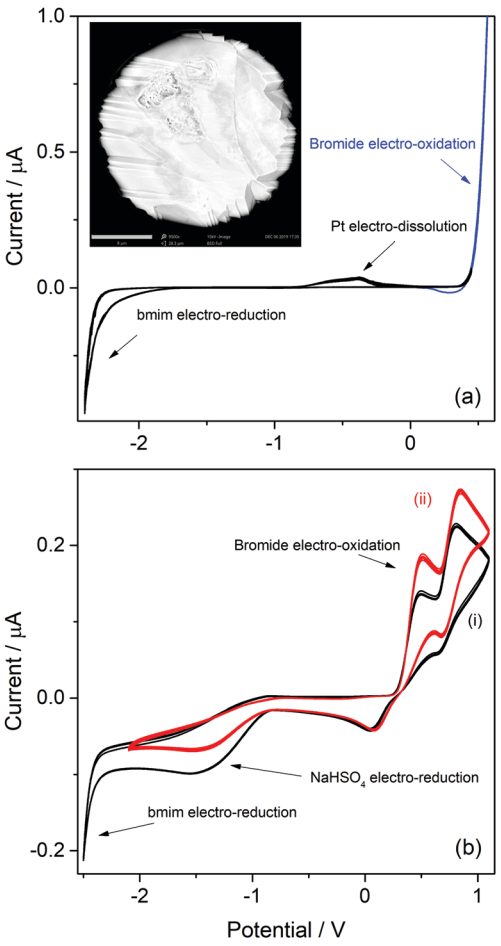

Fig. 1 CVs of a Pt microelectrode in **[bmim]Br** (a) and in **[bmim]HSO_4** (b) before (i) and after (ii) addition of pure **[bmim]Br**. Inset in (a) shows a SEM picture of the Pt microelectrode after the voltammetric analysis (scale bar: 8 μm). T = 80 °C; v = 0.1 V s^{-1}.

range $-1\ V < E < 0\ V$, whose charge slightly increased over the successive scans. Inspection of the Pt ME surface by SEM after being subjected to more than fifty cycles (inset in Fig. 1a) allowed to detect a faceting process of the Pt surface, which is typically caused by electro-dissolution using periodic signals.[41] Thus, it is concluded that this peak was caused by the facile electro-oxidative dissolution of Pt in this highly concentrated bromide solution, presumably leading to dissolved platinum bromide complexes.

Even though there are reports about this behaviour on Au,[42] no similar antecedents were found for this response on Pt. Therefore, these results suggest a potential usefulness of **[bmim]Br** as an electrolyte for the environmentally friendly electrochemical etching of noble metal-based alloys for noble-metal recovering.[43,44] Conversely, the scan toward cathodic direction only shows an exponential current increase at $E < -2.3$ V which, according to previous reports,[38,45] is caused by the electroreduction of the imidazolium cation into the radical imidazol-2-yl, and its further decomposition. In conclusion, the potential window for analyzing possible cathodic discharges from additional proton sources that would be present at the next ILs that are studied in this work is extended down to -2.3 V (as below this limit the **bmim** cation is electro-reduced).

On the other hand, the voltammetric behaviour of a Pt ME in **[bmim]HSO_4** was analyzed, and the CV obtained at 80 °C is shown in Fig. 1b(i). In order to understand this CV, we should keep in mind that this IL has two important differences respect to its bromide analogue. First, the bisulfate counterion is an additional source of protons whose cathodic discharge could occur at potentials above the limit for **bmim** reduction. Second, as it was detailed in the Experimental section, the synthesis of **[bmim]HSO_4** involves the exchange reaction of **[bmim]Br** with $NaHSO_4$, which leads to the formation of NaBr and the ionic pair through reaction (4). As NaBr has very low solubility, it precipitates and is separated by filtration, which allows displacing the exchange equilibrium toward the ionic pair. Taking into account these two aspects, the voltammetric waves in the CV (i) shown in Fig. 1b can be explained. Two oxidation peaks at 0.5 V and 0.8 V are detected, which could be associated to the electro-oxidation of bromide to bromine through a tribromide intermediate (which explains the presence of two peaks).[46,47] These processes reach mass-transport limiting currents, which indicate that the concentration of bromide is low. The most probable source for these low (but detectable) amounts of bromide should be the free **[bmim]Br** that remains in equilibrium with the ionic pair through reaction (4). This was verified by the *in situ* addition of pure **[bmim]Br** to the analyzed IL, which caused an immediate increase of both anodic peaks, as can be seen in Fig. 1b(ii). It should be noted that, in the same way that there is an amount of free **[bmim]Br**, there also may remain some amount of $NaHSO_4$ in equilibrium. Related to that, the cathodic scan shows a mass-transport controlled reduction wave at $E < -0.8$ V, which is tentatively caused by the reduction of this free amount of $NaHSO_4$. This hypothesis was confirmed by the current decrease observed on this wave in Fig. 1b(ii) upon addition of pure **[bmim]Br**, which reacted with part of this free $NaHSO_4$ through reaction (4) and decreased its concentration. At more cathodic potentials ($E < -2.3$ V) an exponential current increase is observed (as it was also detected in **[bmim]Br**), which is likely caused by the electro-reduction of the imidazolium cation.[38,45] It should be noted that the bisulfate anion forming the ionic pair was not electro-reduced over the analyzed potential range, which indicates that the hydrogen atom of this group is strongly tightened into the highly compact structure of the IL, so it would be hardly available for acid catalysis. In summary, the IL **[bmim]HSO_4** conforms a compact arrangement of cations and anions with potential H sources that are deeply involved in the IL structure,[48,49] so their availability is very limited. The only feasible source of protons in this IL is the free sodium bisulfate that remains from the synthesis (together with free **[bmim]Br**).

Voltammetric analysis of [bsmim]HSO_4

As can be seen in the molecular structure of **bsmim** (Table S1, ESI†), the sulfonic acid group in this cation is a potential source of protons for acid catalysis. However, it is not clear how available these hydrogen atoms can be when these groups are involved in the compact IL structure. It was verified in the previously analyzed IL that H atoms from the anion are strongly compromised in building the IL network, so they have a completely different reactivity than the same H atoms in the free anion. If the sulfonic acid groups are usable sources of protons, it should be possible to detect by cyclic voltammetry the hydrogen evolution from these groups. This would constitute strong evidence in order to argue on how accessible these protons are in the IL. However, it should be kept in mind that H-containing free species can also be detected by this technique, as it was the case in the previous analysis of **[bmim]HSO_4** where hydrogen evolution from free $NaHSO_4$ was detected. In this context, Fig. 2a(i) shows a CV measured on a Pt ME in **[bsmim]HSO_4** that was synthesized and purified as described in the Experimental section. This CV shows that in the cathodic scan, there is a significant current increase at $E < -0.5$ V (which is not very negative), indicating the discharge of hydrogen from a protonated species in quite high concentration. Electro-reduction of protons leads to dissolved hydrogen, whose concentration builds up at the electrode surface while it diffuses into the solution. The diffusion rate is affected by the diffusion coefficient of dissolved hydrogen, which in these highly viscous media should be much lower than in aqueous media.[26] Thus, when high current densities are reached, oversaturation of dissolved hydrogen should occur,[50] with the consequent nucleation of hydrogen bubbles at the electrode surface. The size and the dynamic behaviour of these bubbles are governed by the fluid viscosity, among other parameters.[51] The formation and evacuation of bubbles at/from the ME surface generates random variations of the electrode current,[52] which leads to a noisy signal in the CVs shown in Fig. 2. Taking into account that in **[bmim]HSO_4** a similar discharge (but with much smaller current) from free $NaHSO_4$ was detected over this same potential range, it is likely that this current is caused by the discharge of the remaining free acid that was used to neutralize the zwitterions (H_2SO_4 in this case). This free sulfuric acid could be present in the IL not necessarily from remaining amounts that

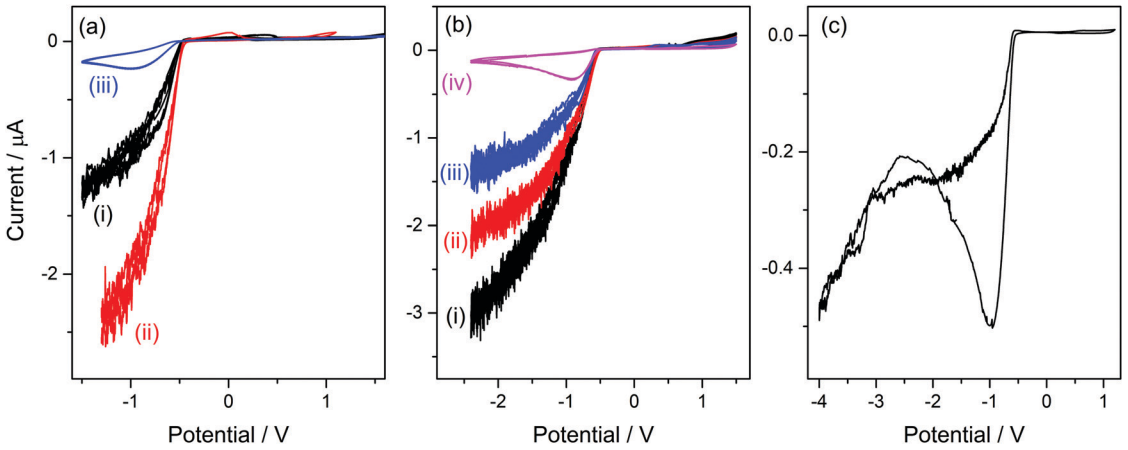

Fig. 2 CVs of a Pt ME in **[bsmim]HSO$_4$** at 80 °C. (a) CVs in **[bsmim]HSO$_4$** purified with two extraction steps (i), in crude **[bsmim]HSO$_4$** (ii), and in **[bsmim]HSO$_4$** purified with six extraction steps (iii). (b) CVs in crude **[bsmim]HSO$_4$** (i), and after three successive additions (18 mg each) of pure **Zbsmim** (ii–iv). (c) Highly cathodic CV in **[bsmim]HSO$_4$** purified with six extraction steps. T = 80 °C; v = 0.1 V s^{-1}.

were not extracted, but also from the reverse displacement of the neutralization equilibrium given by reaction (2). In order to verify this hypothesis, the CVs of samples that were treated in different ways for deliberately changing the presumable amounts of free acid were analyzed. On the one hand, a first strategy was to modify the number of extraction steps used in the purification.

Thus, CVs were measured on three **[bsmim]HSO$_4$** samples with different number of extraction steps, one of them being the IL purified with two extraction steps whose CV was already shown in Fig. 2a(i). It should be noted that the extraction of free H_2SO_4 causes the back displacement of the neutralization equilibrium (reaction (2)), leading to an increase of the concentration of free **Zbsmim**. The CVs measured on an "as-prepared" (or crude) IL (without extraction steps) and on an IL with six extraction steps (where saturation and precipitation of **Zbsmim** was evident) are shown in Fig. 2a(ii) and (iii), respectively. The CV measured in the crude IL shows a significant H_2-evolution current, indicating the presence of a very large amount of remaining free H_2SO_4. The CV taken in the IL with two extraction steps shows that this current is much smaller, being indicative of the good efficiency of the purification method for removing free H_2SO_4. The last CV shows that, even though the repetitive application of extractions (up to six times in this case) led to a decrease of the reduction current to very low levels, it was not possible to eliminate it completely. Moreover, saturation of the IL with **Zbsmim** was evident by detecting its precipitation, which is reasonable taking into account that a decrease of the free acid concentration leads to an increase of free **Zbsmim** concentration by displacement of reaction (2). In fact, once the saturation of the IL with **Zbsmim** was reached, the concentration of free H_2SO_4 became fixed by the equilibrium constant and could not be further decreased.

On the other hand, a second strategy to modify the free acid concentration was to add increasing amounts of pure **Zbsmim** to the crude IL. Thus, CVs measured on a crude **[bsmim]HSO$_4$** IL with different additions of **Zbsmim** are shown in Fig. 2b. A decrease of the current for H_2 discharge is verified for increasing amounts of added **Zbsmim**, which reveals the displacement of reaction (2) generating the ionic pair with the consequent consumption of free H_2SO_4, in consonance with the results of the previous strategy. Results shown in Fig. 2a and b constitute very solid evidences that the IL **[bsmim]HSO$_4$** always contains free H_2SO_4 in concentrations that may vary from a small value in equilibrium with saturated **Zbsmim** to very large values (depending on the number of purification steps). This free H_2SO_4 is the most accessible source of protons in this IL.

The reduction of free H_2SO_4 in samples that contain large amounts of this species involves a significant current that impedes to detect any other parallel reduction process that may occur at $E < -0.5$ V. However, the CVs measured on the IL with the minimum possible amount of free H_2SO_4 shown in Fig. 2a(iii) and b(iv) allowed to confirm that no other species reduces over the analyzed potential range. By extending the cathodic potential limit to more negative values (down to −4 V), as it is shown in Fig. 2c, only one additional cathodic discharge is verified at $E < -2.5$ V. By comparing this response to those measured in **[bmim]**-based ILs that were described previously, it can be inferred that this very cathodic discharge should be associated to the reduction of the imidazolium group.[38,45] Therefore, results shown in Fig. 2c indicate that the protons in the sulfonic acid groups constituting the cations in this TSIL are not electro-reduced over a very wide potential range, similarly to what was already detected for the protons in the bisulfate anions that conform the TSIL network. In summary, it is concluded that even though this TSIL has two potential sources of protons for acid catalysis (sulfonic acid groups at the cation and bisulfate groups at the anion), these protons are strongly bonded to the TSIL macrostructure, possibly playing important roles in keeping its integrity. Thus, the only hydrogen source that is easily available for chemical and electrochemical reactions is the free H_2SO_4 that is at equilibrium with **[bsmim]HSO$_4$** and dissolved **Zbsmim**.

Voltammetric analysis of [bHim]HSO_4

The cation **bHim**, whose structure can be visualized in Table S1 (ESI†), contains a hydrogen atom in position 3 of the imidazole structure (instead of the methyl group in **bmim**), which may be labile enough for participating in acid catalysis. As it was detailed in the Experimental section, the imidazole group receives this hydrogen atom from a strong acid, which in this case is H_2SO_4, through reaction (5). The CV of a Pt ME in **[bHim]HSO_4** (Fig. S1(i) in the ESI†) evidences two cathodic processes. The first wave detected at $E < -0.6$ V corresponds to a mass-transport controlled process, which could be associated to the hydrogen discharge from a very low amount of free H_2SO_4. The addition of pure bim led to the vanishing of this wave (Fig. S1(ii) in the ESI†) due to its reaction with free H_2SO_4, confirming the previous hypothesis. The second discharge at $E < -1.2$ V is an exponential current increase from a species in excess. This is much less cathodic than the **bmim** discharge that occurred at $E < -2.5$ V, and is probably caused by hydrogen evolution from the imidazolic H atom in the **bHim** cation (H3). These results indicate that the IL **[bHim]HSO_4** contains very little amounts of free H_2SO_4 and an additional potential source of hydrogen that, even though is not very labile, could be available for acid catalysis.

Voltammetric analysis of [bsHim]HSO_4

The structure of the cation **bsHim**, which is visualized in Table S1 (ESI†), contains two potential sources of hydrogen, which are the imidazolic hydrogen (H3) and the proton at the sulfonic acid group. On the basis of the previous results obtained on **[bsmim]HSO_4** and on **[bHim]HSO_4**, it seems like the imidazolic hydrogen is easier to reduce than the sulfonic proton, but this should also be verified in this TSIL that contains both sources simultaneously. As it was detailed in the Experimental section, the sulfonic group receives the proton from a strong acid, which in this case is H_2SO_4, through reaction (3), so it is very likely that some amount of free H_2SO_4 may be present. The CV of a Pt ME in **[bsHim]HSO_4** is shown in Fig. 3(i). A large cathodic current is verified at $E < -0.5$ V which, according to previous results, is most likely related to the hydrogen discharge from an excess of free H_2SO_4. This was verified by acquiring CVs after successive additions of increasing amounts of pure **ZbsHim**, causing the consumption of free H_2SO_4 by reaction (3) and the consequent drop of the cathodic currents, as it is observed in CVs (ii) and (iii) of Fig. 3. In fact the CV (iii) was measured in a solution saturated with **ZbsHim**, where an amount of solid zwitterion remained undissolved, so this shows the lowest amount of free H_2SO_4 that can be attained. Precisely in this last solution with such a low content of free H_2SO_4 it was possible to detect a second increase of the cathodic current at $E < -1.3$ V (as it is better observed in the inset graph of Fig. 3). This cathodic process shows up over the same potential range, not very cathodic, of a reduction current that was also observed in **[bHim]HSO_4** (Fig. S1(ii) in the ESI†) and assigned to the discharge of the imidazolic proton. No other cathodic discharges were detected, at least down to a potential of −3 V. Taking into account these evidences, it can be concluded that the protons at the sulfonic acid groups in **[bsHim]HSO_4** are not labile at all, similarly to what was verified in **[bsmim]HSO_4**.

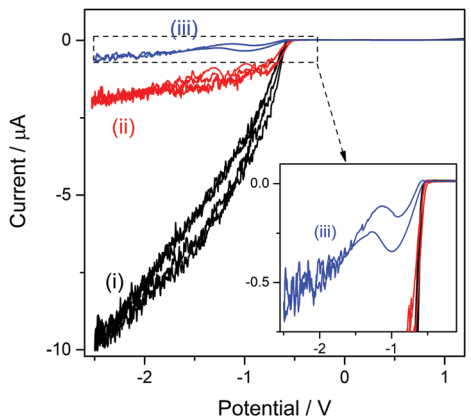

Fig. 3 CVs of a Pt ME in **[bsHim]HSO_4** before (i) and after one (ii) and two (iii) additions of 15 mg of pure **ZbsHim**. Inset graph shows an expanded current scale over the potential interval -2.5 V $\leq E \leq$ 0.0 V. T = 80 °C; v = 0.1 V s^{-1}.

Performance of ILs in a transesterification reaction monitored by UV-vis spectroscopy

Transesterification reactions are being widely studied in the last decades due to their technological application in manufacturing of biodiesel from vegetal oils.[53–55] The recent interest on these processes is mostly focused on seeking alternatives for accomplishing the principles of Green Chemistry, which among other aspects, encourages the use of environmentally friendly and reusable catalysts. Thus, as these TSILs fit into this type of catalysts, our particular interest is to analyze and to understand their catalytic behaviour.

Particularly in this work, we monitored by UV-vis spectroscopy the progress of the reaction of **PNPA** with MeOH leading to **PNP** and methyl acetate (MeAc) through reaction (6), using the four analyzed ILs as catalysts. As **PNP** is a pH indicator that exists at acidic pH values (<6), its detection in protonated form (and not as the phenolate) indicates the presence of an acid reaction medium. The UV-vis spectra of **PNP** and **PNPA** in methanolic solutions containing either of the studied ILs present absorption peaks at ~269 nm (for **PNPA**)[56] and ~310 nm (for **PNP**).[57] The hypsochromic shift of the **PNPA** absorption peak is caused by the lower delocalization of electrons at the oxygen atom in the ester respect to the OH in **PNP**. The absorption maxima of these peaks allows to follow the reaction conversion at different t_R values. Thus, Fig. 4 shows the UV-vis spectra acquired on the reaction media at successive t_R values when using the four studied ILs, as described in the Experimental section. An isosbestic point can be observed in all cases (in the wavelength range between 284 and 288 nm, depending on the used IL), which indicates that the conversion of reagents into products proceeds by a single and quantitative process. It is verified that much shorter t_R values (less than 4 h) are needed to build a significant and invariant concentration of **PNP** (corresponding to almost complete conversion) when using both sulfonic TSILs,

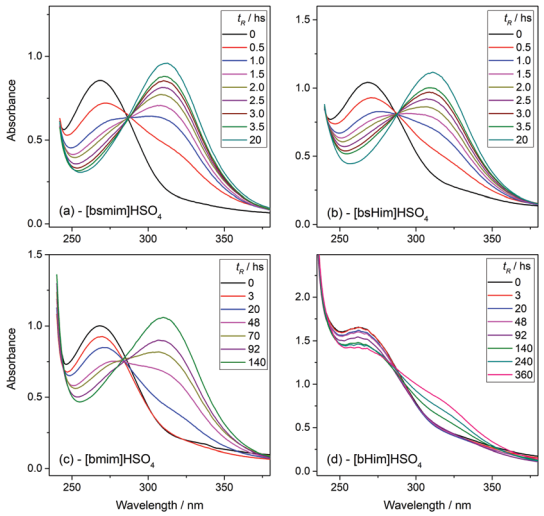

Fig. 4 UV-vis spectra of the reaction media for the transesterification reaction of **PNPA** with MeOH at 25 °C in the presence of **[bsmim]HSO$_4$** (a), **[bsHim]HSO$_4$** (b), **[bmim]HSO$_4$** (c), and **[bHim]HSO$_4$** (d), acquired at different t_R values, as indicated in each graph.

in contrast with the more than 20 h required when using **[bmim]HSO$_4$**. Moreover, in **[bHim]HSO$_4$** the generation of **PNP** is clearly detected only after 48 h. In order to better visualize these differences, the **PNP** concentrations (C_{PNP}) were estimated from these spectra as described in the Experimental section, and the reaction yields were calculated from these concentrations at different t_R values, which are plotted in Fig. 5 for the four ILs. This shows the rapid increase of the reaction yields when using sulfonic TSILs, which tend to the maximum values at t_R in the order of 20 h. These yields contrast with the low values detected when using the respective ILs, which only start to increase after 20 h and are still increasing after 100 h. Moreover, for a more quantitative comparison, apparent rate constants (k^{app}) were calculated from this data assuming a pseudo-first order kinetics respect to **PNPA** concentration (as described in the ESI†), which are shown in Table 1. It is verified that the k^{app} values measured on the ILs are more than

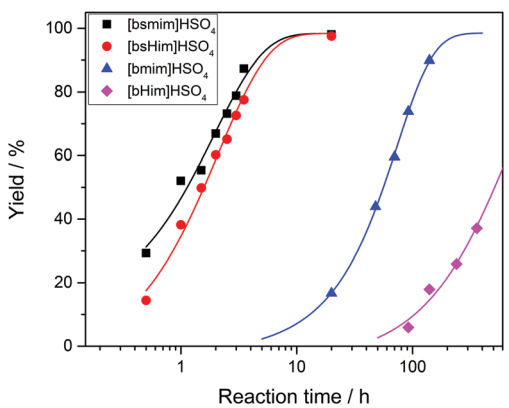

Fig. 5 Yields for the transesterification reaction of **PNPA** with MeOH at 25 °C measured from the UV-vis spectra at different reaction times for the four studied ILs. Lines are drawn for a better trend perception.

Table 1 Apparent pseudo-first order rate constants (k^{app}) calculated for the transesterification reaction of **PNPA** with MeOH at 25 °C using different ILs as acid catalysts

IL	k^{app}/s^{-1}
[bHim]HSO$_4$	$(3.5 \pm 0.2) \times 10^{-7}$
[bmim]HSO$_4$	$(4.2 \pm 0.2) \times 10^{-6}$
[bsHim]HSO$_4$	$(1.21 \pm 0.02) \times 10^{-4}$
[bsmim]HSO$_4$ purified	$(1.56 \pm 0.06) \times 10^{-4}$
[bsmim]HSO$_4$ crude	$(1.25 \pm 0.03) \times 10^{-4}$
[bsmim]HSO$_4$ + **Zbsmim**	$(3.1 \pm 0.1) \times 10^{-5}$
0.1 M H_2SO_4	$(2.14 \pm 0.08) \times 10^{-4}$

two orders of magnitude smaller than those measured on the corresponding sulfonic TSILs. A first hypothesis for such a great catalytic difference between the TSILs and their corresponding ILs is that the catalytic performance would probably be associated to the large amounts of free sulfuric acid (as detected by voltammetry). It was shown that the other potential source of protons at the sulfonic acid group in TSILs is not easily accessible, and would hardly catalyze this reaction. In order to corroborate this hypothesis, the reaction was carried out using a TSIL (**[bsmim]HSO$_4$** in this case) with varying contents of free H_2SO_4. Thus, in addition to the purified **[bsmim]HSO$_4$** that was used in the previous catalytic test, the catalytic performance of other two **[bsmim]HSO$_4$** samples were evaluated. On the one hand, the crude **[bsmim]HSO$_4$** (without purification steps) containing a significant excess of free H_2SO_4 as noted by the CV in Fig. 2b(i), was used as a catalyst with a high content of free H_2SO_4. On the other hand, it was also used the **[bsmim]HSO$_4$** that received successive additions of **Zbsmim** for neutralizing the excess of free H_2SO_4 down to the minimum concentration in equilibrium with saturated **Zbsmim**, as verified by the CV in Fig. 2b(iv).

The reaction yields for each case as a function of t_R are shown in Fig. 6 (complete spectra are provided in the ESI†), and the yields obtained when using pure H_2SO_4 are included as well

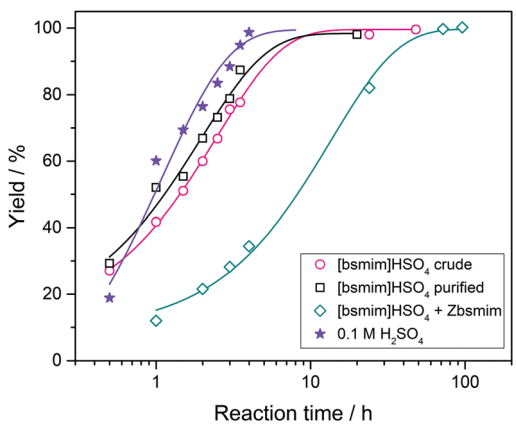

Fig. 6 Yields for the transesterification reaction of **PNPA** with MeOH at 25 °C measured from the UV-vis spectra at different reaction times in the presence of **[bsmim]HSO$_4$** with three different contents of free H_2SO_4. Yields obtained when using 0.1 M H_2SO_4 are also included. Lines are drawn for a better trend perception.

for comparison. Besides, the k^{app} values calculated from this data are tabulated in Table 1. It is verified that the catalytic efficiencies of both TSILs with significant amounts of free H_2SO_4 are similar to that of pure H_2SO_4 (with k^{app} values in the same order of magnitude), where the reaction conversion is almost complete in around 10 h. Thus, it is concluded that the catalytic activity of sulfonic TSILs for this reaction is quite equivalent to that of pure sulfuric acid as long as it contains appreciable amounts of free acid coexisting in equilibrium with the ionic pair. Remarkably, the TSIL with minimum amounts of free H_2SO_4 presented a catalytic activity only slightly lower than the previous cases (with a k^{app} only one order of magnitude smaller), verifying almost complete conversion in around 40 h. These results demonstrate that even though the presence of large amounts of free H_2SO_4 accelerates the reaction to reach high yields in very short times, this is not critical and it takes just a few more hours of reaction for the TSIL to provide the protons that catalyze the reaction to attain complete conversion. The TSIL works as an efficient reservoir for the acid and is capable to dose it on demand to sustain an efficient acid catalysis. The advantages of using sulfonic TSILs instead of pure sulfuric acid are associated to its much safer handling, recycling, and disposal, properties that turn these catalysts very environmentally friendly.

On the other hand, the respective non-sulfonic imidazolic ILs contain very little amounts of free acid, as it was verified by cyclic voltammetry, which leads to very low reaction rates for the catalyzed transesterification reaction at RT. It is evident that the reaction of **PNPA** with MeOH involves the active participation of the free acid (free bisulfate in **[bmim]HSO$_4$** or free sulfuric acid in **[bHim]HSO$_4$**), which should be released by the ionic pairs through a back displacement of the neutralization/exchange reactions that were used to synthesize the ionic pairs (reactions (4) and (5), respectively). Although in **[bmim]HSO$_4$** the reversing of reaction (4) is impeded by the negligible availability of NaBr, the release of H_2SO_4 from **[bHim]HSO$_4$** from the back displacement of reaction (5) should be possible. However, the small amounts of H_2SO_4 verified even at 80 °C in the CVs (Fig. S1(i) in the ESI†) indicates that this reverse process seems to be thermodynamically and kinetically disfavoured, or in other words, the ion pair **[bHim]HSO$_4$** is much more stable than **[bsHim]HSO$_4$**. In spite of that, these catalytic systems could still be useful when operating in high-temperature conditions. In order to analyze this effect, the catalytic performances of the imidazolic ILs were studied by measuring the yields at different reaction times at 60 °C and at 100 °C, verifying a notable increase in the rate to achieve complete conversion, as can be observed in Table 2.

This evidence demonstrates the possibility of using imidazole-based ILs as efficient acid catalysts at temperatures only slightly above ambient conditions. As the synthesis and purification procedures of these ILs are simpler than those of the corresponding sulfonic TSILs (whose syntheses require specific reactants and involve several steps), their use as catalysts can still be a better choice than the respective TSILs in reactive systems where the reaction temperature can be raised.

Table 2 Yields measured for the transesterification reaction of **PNPA** with MeOH using **[bmim]HSO$_4$** and **[bHim]HSO$_4$** at different temperatures and reaction times

	IL	
Temperature (°C)	**[bmim]HSO$_4$**	**[bHim]HSO$_4$**
25	20hs: <20% 92hs: 70–80% 140hs: 90–95%	20hs: <10% 360hs: 30–40%
60	20hs: 80% 48hs: 95–99%	20hs: <30% 92hs: 80% 168hs: 95–99%
100	20hs: 95–99%	—

Conclusions

The global compositions of imidazolic ILs and their derived sulfonic TSILs that use bisulfate as counterion, were analyzed by cyclic voltammetry. The goal was to detect the free species that coexist with the ionic pairs, and to explain on this basis their performances as acid catalysts. The transesterification of **PNPA** with MeOH to produce **PNP** was used as a catalyzed model reaction, as it proved to be a simple and thermodynamically efficient process. From these analyses, it was demonstrated for the first time that the outstanding catalytic activity of sulfonic TSILs is directly associated to the large amounts of free sulfuric acid that are contained within the ILs. However, in conditions of low free acid content, protons that are stored in the sulfonic acid groups constituting the functionalized IL network can be easily delivered through the reverse autoprotolysis equilibria, thus sustaining an acceptable catalytic activity. In addition, a number of other important conclusions about the IL's compositions, electrochemical performances, and reactivities were established, which are described below.

Firstly, it was verified that neither the bisulfate anions conforming the ionic pairs of all the analyzed ILs nor the sulfonic acid groups of the studied TSILs can be electro-reduced. This evidence indicates that these protons may be strongly involved in building the IL's structures and are hardly available for participating in catalytic processes. In fact, the most accessible source of protons in all these ILs is the free acid precursor used for obtaining the bisulfate-based ILs, which remains in equilibrium with the ionic pair in variable amounts. It was verified that both **[bsmim]HSO$_4$** and **[bsHim]HSO$_4$** contained larger amounts of free H_2SO_4 when compared to their respective imidazolic ILs **[bmim]HSO$_4$** and **[bHim]HSO$_4$**, which can explain the higher rates measured on these TSILs when catalyzing the transesterification reaction. The electro-reduction of these protons occurs at potentials that are not very cathodic, so the free acid can function as an effective source of hydrogen for acid catalysis. The amount of free H_2SO_4 may vary depending on the equilibrium constant of the autoprotolysis reaction, the number of extraction steps after synthesis, and the addition of pure base. Besides, the bim-based cations in **[bHim]HSO$_4$** and in **[bsHim]HSO$_4$** contain an additional hydrogen atom at position 3 of the imidazolic ring that can be electro-reduced at

intermediate cathodic potentials, but it has no effect in the catalytic performance of these ILs.

In summary, the catalytic activity at RT of the imidazolic ILs was improved by designing TSILs that incorporate sulfonic acid groups into the imidazolic bases. In principle, the addition of this group was envisaged as an additional source of labile protons that would increase the acidity, but in fact in this work it was proved that these TSILs function as reservoirs for releasing the free acid, which is the actual acid catalyst. The respective imidazolic ILs without the sulfonic acid groups are poor acid catalysts at RT for the tested reaction, but their activity can be significantly improved by increasing the reaction temperature up to 100 °C. Thus, they still can be used as structurally simple efficient catalysts.

Conflicts of interest

There are no conflicts to declare.

Acknowledgements

This work was supported by Universidad Nacional del Litoral (CAI+D 2016 234 and 018), Agencia Santafesina de Ciencia, Tecnología e Innovación (IO 2018 00161), Agencia Nacional de Promoción Científica y Tecnológica (PICT 2017 1340) and CONICET (PUE 229). M. B. M. thanks CONICET for a doctoral fellowship.

Notes and references

1 T. Welton, *Proc. R. Soc. A*, 2015, **471**, 20150502.
2 K. Goossens, K. Lava, C. W. Bielawski and K. Binnemans, *Chem. Rev.*, 2016, **16**, 46430.
3 P. Nancarrow and H. Mohammed, *ChemBioEng Rev.*, 2017, **4**, 106.
4 *Ionic Liquids: Industrial Applications to Green Chemistry*, ed. R. D. Rogers and K. R. Seddon, ACS Symposium Series, Washington, 2002.
5 *Green Industrial Applications of Ionic Liquids*, ed. R. D. Rogers, K. R. Seddon and S. V. Volkov, NATO Science Series: II. Mathematics, Physics and Chemistry, Springer, Dordrecht, 2003, vol. 92.
6 M. J. Earle, J. M. S. S. Esperança, M. A. Gilea, J. N. C. Lopes, L. P. N. Rebelo, J. W. Magee, K. R. Seddon and J. A. Widegren, *Nature*, 2006, **439**, 831.
7 M. Volland, V. Seitz, M. Maase, M. Flores, R. Papp, K. Massonne, V. Stegmann, K. Halbritter, R. Noe, M. Bartsch, W. Siegel, M. Becker and O. Huttenloch, Method for the separation of acids from chemical reaction mixtures by means of ionic fluids, World Pat., WO 03062251, 2003.
8 P. Wasserscheid and W. Keim, *Angew. Chem., Int. Ed.*, 2000, **39**, 3772.
9 A. Wierzbicki and J. H. Davis, Jr., Proceedings of the symposium on advances in solvent selection and substitution for extraction, AIChE, New York, 2000, p. 14F.
10 A. Arfan and J. P. Bazureau, *Org. Process Res. Dev.*, 2005, **9**, 743.
11 R. Giernoth, *Angew. Chem., Int. Ed.*, 2010, **49**, 2834.
12 S. Lee, *Chem. Commun.*, 2006, 1049.
13 Y. Zhao, J. Long, F. Deng, X. Liu, Z. Li, C. Xia and J. Peng, *Catal. Commun.*, 2009, **10**, 732.
14 Y. Q. Cai, G. Q. Yu, C. D. Liu, Y. Y. Xu and W. Wang, *Chin. Chem. Lett.*, 2012, **23**, 1.
15 D.-J. Tao, J. Wu, Z.-Z. Wang, Z.-H. Lu, Z. Yang and X.-S. Chen, *RSC Adv.*, 2014, **4**, 1.
16 H. Ding, W. Ye, Y. Wang, X. Wang, L. Li, D. Liu, J. Gui, C. Song and N. Ji, *Energy*, 2018, **144**, 957.
17 P. Fan, S. Xing, J. Wang, J. Fu, L. Yang, G. Yang, C. Miao and P. Lv, *Fuel*, 2017, **188**, 483.
18 X. Liang and J. Yang, *Green Chem.*, 2010, **12**, 201.
19 Z. Ullah, A. S. Khan, N. Muhammad, R. Ullah, A. S. Alqahtani, S. N. Shah, O. B. Ghanem, M. A. Bustam and Z. Man, *J. Mol. Liq.*, 2018, **266**, 673.
20 P. Berton, S. P. Kelley, H. Wang and R. D. Rogers, *J. Mol. Liq.*, 2018, **269**, 126.
21 S. E. Goodwin, D. E. Smith, J. S. Gibson, R. G. Jones and D. A. Walsh, *Langmuir*, 2017, **33**, 8436.
22 R. Kanzaki, H. Doi, X. Song, S. Hara, S. Ishiguro and Y. Umebayashi, *J. Phys. Chem. B*, 2012, **116**, 14146.
23 M. V. Bravo, J. L. Fernández, C. G. Adam and C. D. Della Rosa, *ChemPlusChem*, 2019, **84**, 919.
24 C. Reichardt and T. Welton, *Solvent Effects in Organic Chemitry*, Wiley-VCH, Weinheim, 4th edn, 2011.
25 *Handbook of Solvents*, ed. G. Wypych, ChemTech Publishing, Toronto, 2001.
26 *Electrochemistry in Ionic Liquids*, ed. A. A. J. Torriero, Springer, Cham, 2015, vol. 1.
27 C. G. Adam and G. Fortunato, *J. Surfactants Deterg.*, 2019, **22**, 501.
28 P. Bonhote, A. P. Dias, N. Papageorgiou, K. Kalyanasundaram and M. Gratzel, *Inorg. Chem.*, 1996, **35**, 1168.
29 C. G. Adam, M. V. Bravo, P. M. E. Mancini and G. G. Fortunato, *J. Phys. Org. Chem.*, 2014, **27**, 841.
30 L. Farkas, O. Schachter and B. H. Vromen, *J. Am. Chem. Soc.*, 1949, **71**, 1991.
31 X. Cui, J. Cai, Y. Zhang, R. Li and T. Feng, *Ind. Eng. Chem. Res.*, 2011, **50**, 11521.
32 Y. Peng, X. Cui, Y. Zhang, T. Feng, Z. Tian and L. Xue, *Appl. Catal., A*, 2013, **466**, 131.
33 Z. Yang, X. Cui, X. Yu, Y. Zhang, T. Feng and H. Liu, *Catal. Lett.*, 2015, **145**, 1281.
34 P. L. Silva, C. M. Silva, L. Guimarães and J. R. Pliego Jr., *Theor. Chem. Acc.*, 2015, **134**, 1591.
35 F. F. Fan, J. L. Fernández, B. Liu, J. Mauzeroll and C. G. Zoski, Ultramicroelectrodes, in *Handbook of Electrochemistry*, ed. C. G. Zoski, Elsevier, Amsterdam, 2007, ch. 6, pp. 189–197.
36 M. Fleischmann and J. N. Hiddleston, *J. Phys. E: Sci. Instrum.*, 1968, **1**, 667.
37 J. A. Bautista-Martinez, L. Tang, J.-P. Belieres, R. Zeller, C. A. Angell and C. Friesen, *J. Phys. Chem. C*, 2009, **113**, 12586.

38 R. Michez, T. Doneux, C. Buess-Herman and M. Luhmer, *ChemPhysChem*, 2017, **18**, 2208.
39 A. García-Mendoza and J. C. Aguilar, *Electrochim. Acta*, 2015, **182**, 238.
40 C. L. Bentley, A. M. Bond, A. F. Hollenkamp, P. J. Mahon and J. Zhang, *J. Phys. Chem. C*, 2014, **118**, 22439.
41 R. M. Cerviño, A. J. Arvía and W. Vielstich, *Surf. Sci.*, 1985, **154**, 623.
42 P. H. Qi and J. B. Hiskey, *Hydrometallurgy*, 1993, **32**, 161.
43 C. Deferm, J. Hulsegge, C. Möller and B. Thijs, *J. Appl. Electrochem.*, 2013, **43**, 789.
44 M. Balva, S. Legeai, N. Leclerc, E. Billy and E. Meux, *ChemSusChem*, 2017, **10**, 2922.
45 R. Michez, J. Vander Steen, T. Doneux, M. Luhmer and C. Buess-Herman, *Electrochim. Acta*, 2018, **270**, 434.
46 G. D. Allen, M. C. Buzzeo, C. Villagrán, C. Hardacre and R. G. Compton, *J. Electroanal. Chem.*, 2005, **575**, 311.
47 M. Tariq, *Z. Phys. Chem.*, 2019, **234**, 295.
48 J. Dupont and P. A. Z. Suarez, *Phys. Chem. Chem. Phys.*, 2006, **8**, 2441.
49 J. Dupont, *J. Braz. Chem. Soc.*, 2004, **15**, 341.
50 S. Lubetkin, *Electrochim. Acta*, 2002, **48**, 357.
51 Q. Chen, L. Luo, H. Faraji, S. W. Feldberg and H. S. White, *J. Phys. Chem. Lett.*, 2014, **5**, 3539.
52 J. Zhou, Y. Zu and A. J. Bard, *J. Electroanal. Chem.*, 2000, **491**, 22.
53 N. K. Patel and S. N. Shah, Biodiesel from plant oils, in *Food, Energy, and Water*, ed. S. Ahuja, Elsevier, Amsterdam, 2015, ch. 11, pp. 277–307.
54 D. A. Kotadia and S. S. Soni, *Monatsh. Chem.*, 2013, **144**, 1735.
55 M. Koberg and A. Gedanken, Using Microwave Radiation and SrO as a Catalyst for the Complete Conversion of Oils, Cooked Oils, and Microalgae to Biodiesel, in *New and Future Developments in Catalysis*, ed. L. SuibS, Elsevier, Amsterdam, 2013, ch. 9, pp. 209–227.
56 https://spectrabase.com/spectrum/LQ5aBGZth9Q.
57 https://spectrabase.com/spectrum/FNHzrlrR4wS.